Strain-induced superconducting pair density wave states in graphene

Feng Xu,[1] Po-Hao Chou,[2] Chung-Hou Chung,[3] Ting-Kuo Lee,[4] and Chung-Yu Mou[2,4,5]

[1]*School of Physics and Telecommunication Engineering, Shaanxi University of Technology, Hanzhong 723001, China*

[2]*Center for Quantum Technology and Department of Physics, National Tsing Hua University, Hsinchu 30043, Taiwan, 300, Republic of China*

[3]*Electrophysics Department, National Chiao-Tung University, HsinChu, Taiwan, Republic of China*

[4]*Institute of Physics, Academia Sinica, Nankang 115, Taiwan, Republic of China*

[5]*Physics Division, National Center for Theoretical Sciences, Hsinchu 30013, Taiwan, Republic of China*

(Received 8 August 2018; revised manuscript received 7 October 2018; published 2 November 2018)

Graphene is known to be nonsuperconducting. However, surprising superconductivity is recently discovered in a flat band in a twisted bilayer graphene. Here, we show that superconductivity can be more easily realized in topological flat bands induced by strain in graphene through periodic ripples. Specifically, it is shown that by including correlation effects, the chiral d-wave superconductivity can be stabilized under strain even for slightly doped graphene. The chiral d-wave superconductivity generally coexists with charge density waves (CDW) and pair density waves (PDW) of the same period. Remarkably, a pure PDW state with doubled period that coexists with the CDW state is found to emerge at a finite-temperature region under reasonable strain strength. The emergent PDW state is shown to be superconducting with nonvanishing superfluid density, and it realizes the long-sought-after superconducting states with nonvanishing center-of-mass momentum for Cooper pairs.

DOI: 10.1103/PhysRevB.98.205103

I. INTRODUCTION

The issue of what alternative forms of superconducting states other than the BCS superconducting states can be realized has been one of the main drives for searching unconventional superconductivity in condensed matter. In the high-temperature superconductivity discovered in cuprates, it is now widely accepted that both the mechanism and the pairing symmetry are different from those in the conventional superconductivity [1]. Furthermore, while the Cooper pairs have zero center-of-mass momentum in the conventional superconductivity and the charge density waves (CDW) are usually considered as being incompatible with this property [2], it is also realized that both CDW and pair density waves (PDW) that break translational symmetry are intertwined and can even coexist with the superconducting order [1,3,4]. More recently, it is put forth that while in conventional superconductors, the critical temperature is limited by the Debye frequency ω_D through the relation for critical temperature $k_B T_c = \hbar\omega_D e^{-1/Ng}$, in an extreme limit when the electronic band is dispersionless and becomes a flat band, the divergence of the density of states N near the Fermi energy leads to enhanced critical temperature that is proportional to the electron-phonon coupling constant g, i.e., $k_B T_c = g/2$ [5]. The flat-band superconductivity is based on naive extrapolation of the BCS theory. In real materials, however, decreasing electronic bandwidth enhances onsite Coulomb interaction and may induce other instabilities such as CDW, antiferromagnetic order, ferromagnetism [6], etc. Indeed, as-grown graphene is known to be nonsuperconducting. However, in a recent experiment, superconductivity with strong correlation effects is discovered in a flat band arising in slightly twisted bilayer graphene [7,8]. The discovered flat-band superconductivity indicates that graphene may host unconventional superconductivity under appropriate conditions.

In this paper, we explore superconducting phases in flat bands formed by an alternative way in graphene. Unlike the flat band in twisted bilayer graphene that requires fine-tuning of the twisted angle, here flat bands are formed topologically by strain and can be robustly induced as Landau levels because of the corresponding pseudomagnetic field generated by the strain [9]. Experimentally, flat bands in strained graphene have been observed with the strain being imposed or engineered by external stretching or periodic ripples [9–11]. Here, by including correlation effects in graphene under periodic strain, it is shown that unconventional superconducting states with chiral d-wave symmetry can be stabilized even in slightly doped graphene. Furthermore, because of the periodicity introduced by strain, we find that the chiral d-wave superconductivity generally coexists with CDW and PDW of the same period. Remarkably, a pure PDW state with doubled period that coexists with CDW is found to emerge at a finite-temperature region under reasonable strain strength. The emergent PDW state is shown to be superconducting with nonvanishing superfluid density and realizes the long-sought-after superconducting states with nonvanishing center-of-mass momentum for Cooper pairs [12].

II. THEORETICAL MODEL AND RESULTS

We start by considering the graphene under periodic strain. As shown in Fig. 1(b), the strain can be induced by ripple with fixed period L or by external stretching. The strain generally induces changes of hopping amplitudes t through the change of bond lengths δ_1, δ_2, and δ_3 as $t_i = t\exp[-3.37(|\vec{e}_i|/a - 1)]$ [13] [see Fig. 1(a)]. Here $t \approx 2.8$ eV is the equilibrium hopping amplitude, $a = 1.42$Å is the equilibrium bond length, and $\vec{e}_i$ are three deformed nearest-neighbor vectors whose corresponding undeformed vectors are $\vec{e}_1^0 = \frac{a}{2}(1, \sqrt{3})$, $\vec{e}_2^0 = \frac{a}{2}(1, -\sqrt{3})$, and $\vec{e}_3^0 = -a(1, 0)$. In the simplest realization,

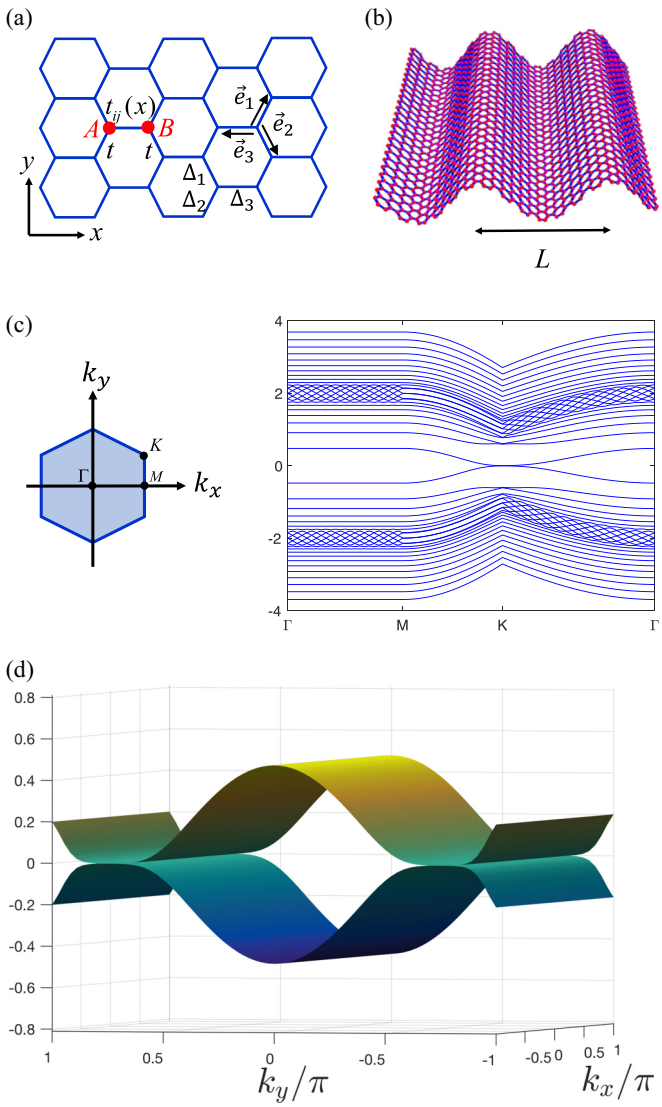

FIG. 1. Topological flat bands in strained graphene: (a) Strain-induced change of hopping amplitude. Here $t_{ij}(x) = t[1 + \alpha\cos(Qx_i)]$ with i denoting site A and j denoting site B. Δ_i represents three superconducting pairing amplitudes. (b) Schematic plot of the ripple with period L. (c) Plot of energy bands for $\alpha = 0.8$ and $L = 24$ in the Brillouin zone of unstrained graphene. (d) Extension of zero-energy flat band (along the M-K direction) in strained graphene with $\alpha = 0.8$ and $L = 24$.

we shall keep e_1 and e_2 fixed and deform e_3 with the period L [14]. The corresponding change in the hopping amplitude along the horizontal bond is given by

$$t_{ij} = t[1 + \alpha\cos(Qx_i)], \tag{1}$$

where x labels the position of the left-hand site [A in Fig. 1(a)] of the bond AB and the $Q = 2\pi/L$ is the wave vector associated with the strain. For ripples with the wavelength being in the nanometer regime, $0 < \alpha \leqslant 0.5$ and $L = 0.1$–10 nm [9,11].

The tight-binging Hamiltonian under strain is given by

$$H_0 = -\sum_{i,j=1,2,\sigma} t c^\dagger_{i,\sigma} c_{i-\vec{e}_j,\sigma} - \sum_{i,\sigma} t(x_i) c^\dagger_{i,\sigma} c_{i-\vec{e}_3,\sigma} + \text{H.c.}, \tag{2}$$

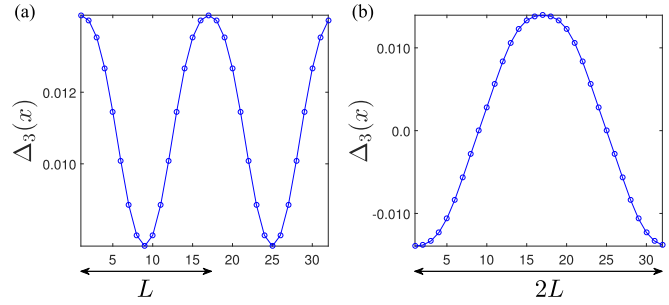

FIG. 2. Numerical solutions that illustrate the pair density wave with an anomalous period. Here pairing amplitudes Δ_i are defined in Fig. 1, $\alpha = 0.025$, and $\delta = 0.122$. (a) Δ_3 of the ground state exhibits a uniform order plus a component that oscillates with the same period L of the strain (or period of L/n with n being positive integer). (b) Δ_3 of the metastable state close to the ground state exhibits anomalous period of $2L$. Here, by assuming translational invariance in the y direction, mean fields χ_{ij} and Δ_{ij} on each bond in real space are solved self-consistently in a 32×32 lattice with $J/t = 1$.

where i labels sub-lattice A, $t(x_i) = t_{i,i-\vec{e}_3}$, and $c_{i,\sigma}$ annihilates an electron with spin σ on site i. The typical effect of strain on the energy spectrum of electrons is shown in Fig. 1(c). It is seen that energy bands get flattened. In a large period limit, these flat bands near the Dirac point coincide with the Landau levels as a result of the strain-induced pseudomagnetic fields [15]. For general periodic perturbation of hopping amplitudes given by Eq. (1), the vector potential associated with the pseudomagnetic field is given by $A_x = \sqrt{3}(t_{i_1} - t_{i_2})/2v_F$, $A_y = (t_{i_1} + t_{i_2} - 2t_{i_3})/2v_F$ [16], where t_{i_n} $(n = 1, 2, 3)$ are hoppping amplitudes along $\vec{e}_n$ at site i (see Fig. 1(a)). Hence, for the deformed hopping amplitude of Eq. (1), we have $A_x = 0$ and $A_y = -t\alpha\cos(Qx)/v_F$. The linearized Hamiltonian near the K point can be written as

$$H_q = \hbar v_F \begin{pmatrix} 0 & -i\frac{d}{dx} + i(q_y - A_y) \\ -i\frac{d}{dx} - i(q_y - A_y) & 0 \end{pmatrix}, \tag{3}$$

where q_y is the deviation of the wave vector $\mathbf{k}$ from K. Clearly, for large L (small Q), H_q supports zero-energy solutions near $q_y - A_y(x) = 0$ with the eigenstate ψ_0 being given by

$$\psi_0 = N \begin{pmatrix} \exp^{-\int_{x_0}^{x}[q_y - A_y(x)]dx} \\ 0 \end{pmatrix}, \quad \text{for } \frac{d}{dx}[q_y - A_y(x)] > 0 \tag{4}$$

or

$$\psi_0 = N \begin{pmatrix} 0 \\ \exp^{-\int_{x_0}^{x}[q_y - A_y(x)]dx} \end{pmatrix}, \quad \text{for } \frac{d}{dx}[q_y - A_y(x)] < 0, \tag{5}$$

where N is a normalization constant and x_0 is a root to $q_y - A_y(x) = 0$. It is clear from the above solution that only when $|q_y| \leqslant t\alpha/v_F$ is satisfied, x_0 exists so that zero-energy solutions exist [17]. This results a flat region along q_y direction (M-K) as illustrated in Fig. 2(d).

To include correlation effects in flat bands, we consider graphene near half-filling with the averaged electron

density being less than 1. The appropriate model is to include the Hubbard interaction between electrons, $H_U = H_0 + U\sum_{i,\sigma}\hat{n}_{i\uparrow}\hat{n}_{i\downarrow}$. In the strong interacting limit when **U** is large, the Hilbert space of the ground state is energetically confined to the singly occupied space described by an effective t-J model given by [18]

$$H = P_G\left[H_0 + \sum_{\langle ij\rangle} J_{ij}\left(\vec{S}_i\cdot\vec{S}_j - \frac{1}{4}n_i n_j\right)\right]P_G. \quad (6)$$

Here t is the deformed hopping amplitude $t_{ij}(x_i)$, J is the antiferromagnetic coupling J_{ij}, and $P_G = \Pi_i(1-n_{i\uparrow}n_{i\downarrow})$ is the Gutzwiller projection operator that projects out states with doubly-occupied sites. $\vec{S}$ and n are spin and number operators for electrons respectively. The antiferromagnetic (AF) coupling, given by $J_{ij} = 4t_{ij}^2/U$, now acquires spatial dependence through the deformed hopping amplitude $t_{ij}(x_i)$.

To investigate possible phases that arise with the given Hamiltonian H, we resort to the slave-boson method, in which the no-double-occupancy constraint is implemented by expressing the electron operator as $c_{i\sigma} = b_i^\dagger f_{i\sigma}$ with b_i being the holon carrying the charge and $f_{i\sigma}$ being the spinon carrying the spin [19,20]. The no-double-occupancy constraint is satisfied by requiring $\sum_\sigma f_{i\sigma}^\dagger f_{i\sigma} + b_i^\dagger b_i = 1$. Following Ref. [19], in the mean-field approximation, b_i is replaced by $\langle b_i\rangle = \sqrt{\delta_i}$ with $\delta_i = 1 - n_i$ being the hole density at the i site. The AF interaction is further decoupled as $\vec{S}_i\cdot\vec{S}_j - \frac{1}{4}\hat{n}_i\hat{n}_j \to -\frac{3}{8}(\hat{\chi}_{ij}^\dagger\hat{\chi}_{ij} + \hat{\Delta}_{ij}^\dagger\hat{\Delta}_{ij})$, where $\hat{\chi}_{ij}^\dagger = f_{i\uparrow}^\dagger f_{j\uparrow} + f_{i\downarrow}^\dagger f_{j\downarrow}$ and $\hat{\Delta}_{ij}^\dagger = f_{i\uparrow}^\dagger f_{j\downarrow}^\dagger - f_{i\downarrow}^\dagger f_{j\uparrow}^\dagger$. Taking the mean-field approximation of the decoupled AF interaction, the mean-field Hamiltonian is given by

$$H_{MF} = \left[\sum_{\langle ij\rangle,\sigma} -\tilde{t}_{ij} f_{i\sigma}^\dagger f_{j\sigma} + \sum_{\langle ij\rangle}\tilde{\Delta}_{ij}^0(f_{i\uparrow}^\dagger f_{j\downarrow}^\dagger - f_{i\downarrow}^\dagger f_{j\uparrow}^\dagger)\right] + \text{H.c.} - \sum_{\langle ij\rangle}\tilde{J}_{ij}\left(|\chi_{ij}|^2 + |\Delta_{ij}^0|^2\right). \quad (7)$$

Here $\chi_{ij} = \langle\hat{\chi}_{ij}\rangle$, $\Delta_{ij}^0 = \langle\hat{\Delta}_{ij}\rangle$, $\tilde{t}_{ij} = \sqrt{\delta_i\delta_j}t_{ij} - \tilde{J}_{ij}\chi_{ij}$ is the effective hopping strength, $\tilde{\Delta}_{ij}^0 = \tilde{J}_{ij}\Delta_{ij}^0$, and $\tilde{J}_{ij} = -3J_{ij}/8$. χ_{ij} and Δ_{ij} are solved self-consistently through the equations $\chi_{ij} = \langle\hat{\chi}_{ij}\rangle$ and $\Delta_{ij}^0 = \langle\hat{\Delta}_{ij}\rangle$ with $\langle\hat{\chi}_{ij}\rangle$ and $\langle\hat{\Delta}_{ij}^0\rangle$ being numerically computed by using the mean-field Hamiltonian H_{MF}. Note that Δ_{ij}^0 (and thus $\tilde{\Delta}_{ij}^0$) is the average of spinon pairing operator, $\hat{\Delta}_{ij}$, and hence it is not the superconducting amplitude. The superconducting pairing amplitude is the pairing amplitude of electrons and is given by $\Delta_{ij} = \sqrt{\delta_i\delta_j}\Delta_{ij}^0 \approx \delta\Delta_{ij}^0$ with $\tilde{\Delta}_{ij} = \tilde{J}_{ij}\Delta_{ij}$. The superconducting transition temperatures is thus obtained by rescaling the transition temperature for the spinon gap by the average doping δ. Finally, we note that H_{MF} is essentially the same as the renormalized mean-field Hamiltonian [21] obtained by using the Gutzwiller approximation [22] except that the hopping amplitude t_{ij} and the AF coupling J_{ij} are replaced by $g_t t_{ij}$ and $g_s J_{ij}$ with $g_t = 2\sqrt{\delta_i\delta_j}$ and $g_s = 4$. Hence, both the slave-boson method and the mean-field theory based on the Gutzwiller approximation yields similar results.

To analyze superconducting states in the strain, we define pairing orders on nearest neighboring bonds to any lattice point as shown in Fig. 1(a) (the same definition applies to χ_{ij} as well). Note that $\Delta_2 = \Delta_1^*$ is satisfied due to the C_3 rotational symmetry. There are three pairing symmetries in compatible with the symmetry of graphene [23]: extended s-wave, $d_{x^2-y^2} + id_{xy}$, and $d_{x^2-y^2} - id_{xy}$. They can be expressed in terms of pairing amplitudes along three bonds as $\Delta_s(x) = \frac{1}{\sqrt{3}}[\Delta_1(x) + \Delta_2(x) + \Delta_3(x)]$, $\Delta_{d_{x^2-y^2}}(x) = \frac{1}{\sqrt{6}}[2\Delta_3(x) - \Delta_1(x) - \Delta_2(x)]$, and $\Delta_{d_{xy}}(x) = \frac{1}{\sqrt{2}}\text{Im}[\Delta_1(x) - \Delta_2(x)]$. In the absence of strain, the uniform chiral d-wave state, $d_{x^2-y^2} \pm id_{xy}$, is found to be the superconducting ground state for $J \geqslant 1$ [23]. In the presence of strain, we solve mean fields χ_{ij} and Δ_{ij} on each bond in real space self-consistently. Figures 2(a) and 2(b) show typical convergent values for $\Delta_3(x)$. Because of the imposed periodicity by the strain, one expects that in addition to the uniform $\chi_{ij} = \chi$ and $\Delta_{ij} = \Delta$, χ_{ij} and Δ_{ij} of period L/n with $n = 1, 2, 3, \ldots$ (wave vector $= nQ$) are also present and coexist with the uniform orders. This is clearly seen in Fig. 2(a), in which Δ_3 exhibits period of L. However, as indicated in Fig. 2(b), in addition to period L, mean-field orders with anomalous period of $2L$ emerge in certain regime of the strain amplitude α.

To further explore the density waves with anomalous period of $2L$, we solve superconducting phases of the graphene in zero temperature by classifying phases with or without the period of $2L$ (wave vector $Q/2$) as the following:

phase I: Δ_s, $\Delta_{d_{x^2-y^2}\pm id_{xy}}$ (uniform orders), $\Delta_s(nQ)$, $\Delta_{d\pm id}(nQ)$, $\chi(nQ)$, and $\rho(nQ)$

phase II: $\Delta_{d_{xy}}$, $\Delta_{d_{xy}}(nQ)$, $\chi(nQ)$, $\rho(nQ)$, $\Delta_s(Q/2)$, $\Delta_{d_{x^2-y^2}}(Q/2)$, and $\chi_1(Q/2)$.

Here $\rho(nQ)$ represents the onsite charge density wave $\sum_i n_i e^{inQx_i}$ and $\chi(Q/2)$ represents the bond charge density wave $\sum_i \chi_{ij}e^{iQx_i/2}$. The phase diagram is shown in Fig. 3(a). It is seen that there is a large region with moderate strain for $\alpha \approx 0.1$–0.3 in which density waves with period of $2L$ (phase II) can be stabilized. For a given doping δ, Fig. 3(b) shows that as the strain increases, quantum phase transitions occur with the change of superconducting orders being discontinuously across phase boundaries.

To understand the emergence of orders with wave vector $Q/2$ (period $= 2L$), we consider possible couplings between the charge density wave, the pair density wave, and the uniform superconducting order Δ. The energy terms in the free energy must conserve the momentum, i.e., the total momentum must vanish. In addition, the U(1) symmetry should be respected. As a result, we find that the lowest order couplings in the free energy are of the form [24] $\rho(Q)\Delta^*(Q/2)\Delta(-Q/2)$, $\rho(Q)\Delta^*\Delta(-Q)$, $|\chi(Q/2)|^2|\Delta(Q)|^2$, and $|\chi(Q)|^2|\Delta(Q)|^2$. In these lowest coupling terms, the mechanism for the emergency of finite Cooper pair momentum is due to the momentum conservation. For instance, in the lowest order of the coupling term, $\rho(Q)\Delta^*(Q/2)\Delta(-Q/2)$, the momentum Q carried by CDW is conserved by creating two Cooper pairs with momentum $-Q/2$. The emergent Cooper pair order with momentum $Q/2$ is generally not stable and has to be stabilized as the minimum of the free energy. For graphene under the strain given by Eq. (1), the induced charge density wave $\rho(Q)$ is proportional to the deformation of hopping amplitude $\delta t \equiv t\alpha$. Hence the minimum of the free energy is driven by the couplings $a(Q)\delta t(Q)\Delta^*(Q/2)\Delta(-Q/2) +$

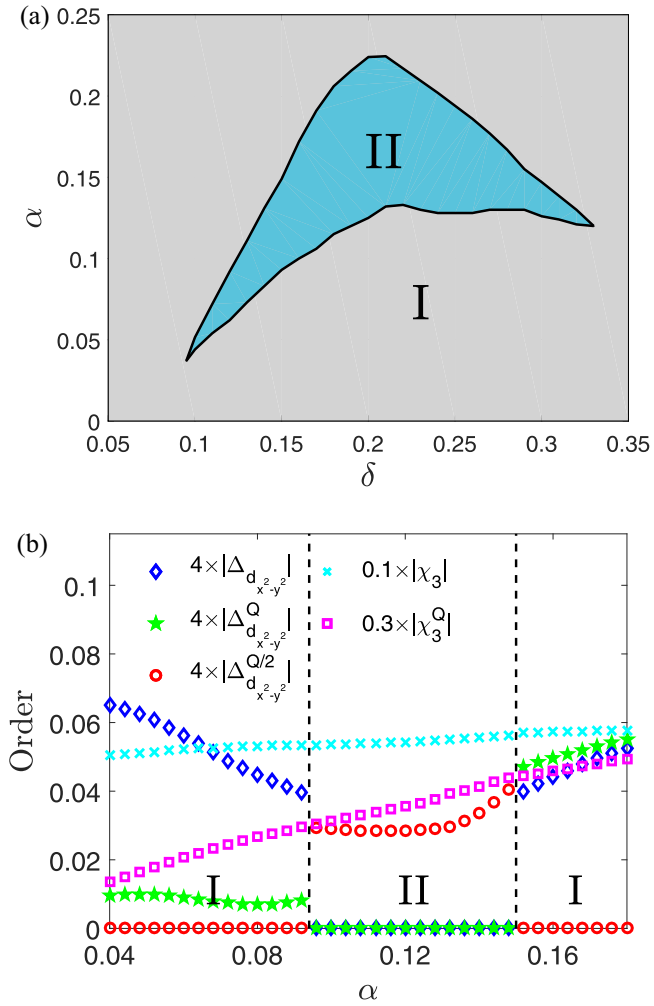

FIG. 3. Superconducting phases of strained graphene at zero temperature with $L = 16$ and $J/t = 1$ (a) Phase diagram in the parameter space of doping δ and strain α. Here in phase I, only orders of integer multiple of wave vector $Q = 2\pi/L$, i.e., nQ, appear. In phase II, orders with wave vector $Q/2$ coexist with orders with wave vector nQ. (b) Quantum phase transitions of mean-field orders for $\delta = 0.15$. It is seen that superconducting orders change discontinuously across phase boundaries.

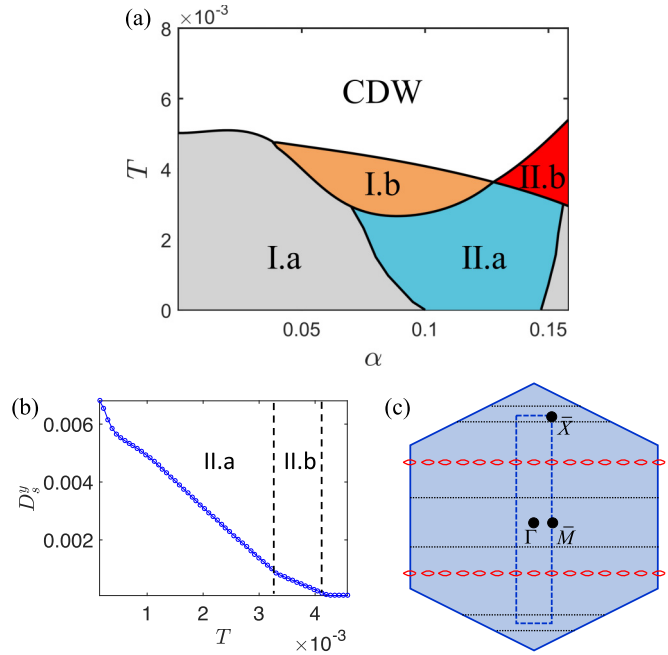

FIG. 4. Superconducting phases of strained graphene at finite temperatures with $L = 16$, $J/t = 1$, and $\delta = 0.15$. (a) Distinct phases with different superconducting orders (see text for more details) at finite temperatures. Here phase II.b is a pure superconducting PDW state with nonzero center-of-mass momentum for Cooper pairs and coexists with the CDW order. (b) Superfluidity weight along a cut from phase II.a to the CDW phase with $\alpha = 0.14$. The nonvanishing D_y implies that the pure PDW state in phase II.b is superconducting. (c) Nodal rings (indicated by red color) of quasiparticles in phase II.b. In addition to nodal rings, flat bands marked by black solid lines are also on the Fermi surface in the normal states without pairing density waves.

$b(Q)|\delta t(Q)|^2|\Delta(Q)|^2$. Here the coefficients $a(Q)$ and $b(Q)$ are negative [25] so that both $\Delta(Q/2)$ and $\Delta(Q)$ can be stabilized for sufficiently large α.However, because of different dependences on α, $\Delta(Q/2)$ and $\Delta(Q)$ compete with each other and eventually $\Delta(Q/2)$ wins, resulting in the emergence of phase II as an intermediate phase.

At finite temperatures, the competition of different superconducting orders lead to more complicated phase diagrams as shown in Fig. 4(a). Here orders emerging in different phases are the following:

phase I.a: Δ_s, $\Delta_{d\pm id}$, $\Delta_s(nQ)$, $\Delta_{d\pm id}(nQ)$, $\chi(nQ)$, and $\rho(nQ)$,

phase I.b: $\Delta_{d_{xy}}$, $\Delta_{d_{xy}}(nQ)$, $\chi(nQ)$, and $\rho(nQ)$,

phase II.a: $\Delta_{d_{xy}}$, $\Delta_{d_{xy}}(nQ)$, $\chi(nQ)$, $\rho(nQ)$, $\Delta_s(Q/2)$, $\Delta_{d_{x^2-y^2}}(Q/2)$, and $\chi_1(Q/2)$,

phase II.b: $\rho(nQ)$, $\chi(nQ)$, $\Delta_s(Q/2)$, and $\Delta_{d_{x^2-y^2}}(Q/2)$.

Here, for small α, when going from phase I.a to phase I.b, superconducting order Δ_i becomes pure imaginary and only Δ_1 and Δ_2 survive, while for large α, going from phase II.a to phase II.b, $\Delta_{d_{xy}}(Q)$ and $\chi_1(Q/2)$ disappear. The driving coupling for disappearance of $\Delta_{d_{xy}}(Q)$ and $\chi_1(Q/2)$ is the coupling $|\chi(Q/2)|^2|\Delta(Q)|^2$. Remarkably, because of this coupling, we see that a pure PDW state that coexists with the CDW order emerges at some finite temperature with moderate strain $\alpha \gtrsim 0.125$ (phase II.b). Furthermore, as shown in Fig. 4(b), by computing the superfluid weight [26], we find that phase II.b is superconducting, in contrast to the CDW state with vanishing superfluid weight. Similar to the PDW state observed in high-Tc cuprates in which the quasiparticle excitations are gapless with Fermi arcs displayed at finite temperatures [4], here phase II.b is also gapless with nodal rings (red curves) as shown in Fig. 4(c). The exact location of the nodal ring can be exhibited in the corresponding energy spectrum, which is plotted in Figs. 5(a) and 5(b), showing the energy spectrum of the quasiparticle excitation along the path Γ-$\bar{M}$-$\bar{X}$-Γ. Here the enlargement of Fig. 5(a) for $E_k \sim 0$ is shown in Fig. 5(b), indicating the location of the nodal ring in going from $\bar{M}$ to $\bar{X}$.

Note that without flat bands, it is generally more difficult to have pair of states near the Fermi surface to satisfy the

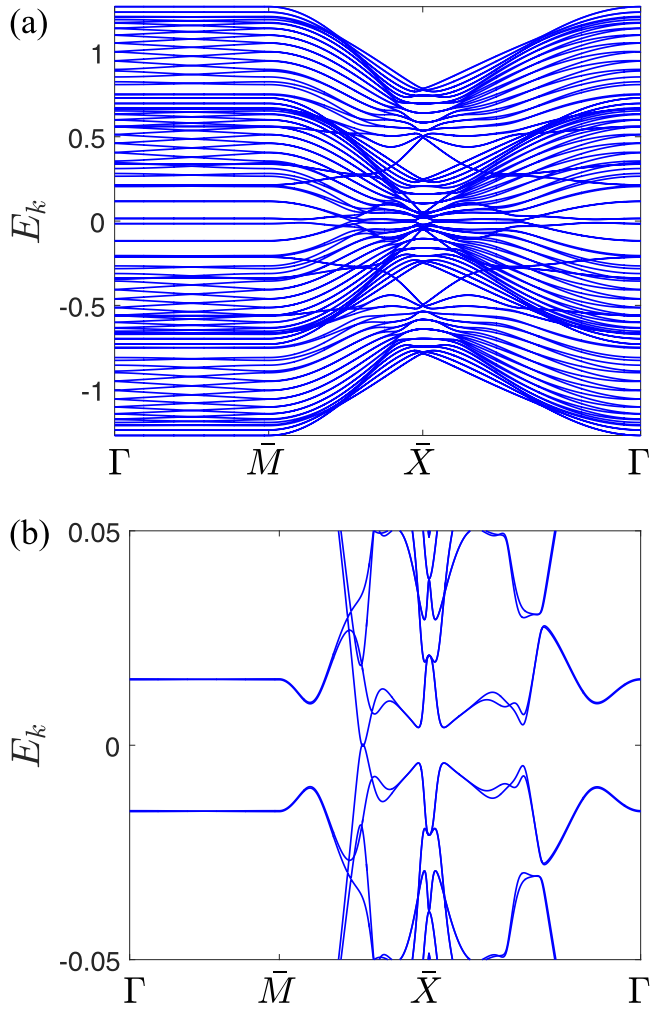

FIG. 5. (a) Quasiparticle excitations in phase II.b. (b) Enlargement of the energy spectrum near $E_k \sim 0$ shown in panel (a). Here $\bar{M}$ and $\bar{X}$ are points at the boundary of reduced Brillouin zone shown in Fig. 4(c) in the text. It is seen that E_k only vanishes at nodal points (from the nodal rings) in going from $\bar{M}$ to $\bar{X}$.

condition that the total momentum is $Q/2$. Hence, density for pair of states near the Fermi surface with total momentum $Q/2$ is low. In the presence of flat bands, it is much easier to satisfy the condition with the total momentum being $Q/2$ as the energy does not depend on the momentum. Therefore, flat bands help in stabilizing the Cooper pair with momentum $Q/2$. This is illustrated in Fig. 4(c), which shows flat bands (black solid lines) on the Fermi surface in the normal state are gapped out due to pairing of electrons with center-of-mass momentum being $Q/2$, while the same pairing is not possible for ring-shape Fermi surfaces, leaving nodal rings as gapless excitations in phase II.b. Phase II.b is thus a unique realization of the long-sought-after superconducting state with nonvanishing center-of-mass momentum for Cooper pairs.

III. DISCUSSION AND SUMMARY

In summary, while superconductivity is discovered to be realized in a flat band in a twisted bilayer graphene, we find that the same chiral d-wave superconductivity can be also realized in topological flat bands induced by strain in graphene through periodic ripples. The stabilization of chiral d-wave superconductivity is through the enhancement of the correlation effect in flat bands. As a result, even for slightly doped graphene, the graphene can be turned into a chiral d-wave superconductor by applying strain. The uniform chiral d-wave superconductivity generally coexists with the CDW order and chiral PDW order. At finite temperatures, it is further found that a pure superconducting PDW state with coexisting CDW emerges in graphene under moderate strain strength. The emergent pure superconducting PDW state is the realization of the long-sought-after superconducting state with nonvanishing center-of-mass momentum for Cooper pairs.

Finally, we discuss the feasibility of realizing the superconducting PDW state and the experimental features that can be observed. First, distinguishing the superconducting PDW state from other superconducting state can be generally detected by using the scanning tunneling microscope. One expects that the energy gap observed in the differential conductance measurement depends on the position and exhibits oscillatory behavior. For the feasibility of realizing the superconducting PDW state, so far our analysis has focused on nanoscale ripples (wavelength from 0.1 to 10 nm), which have been observed experimentally [9,10]. It is known that the generation of flat bands by ripple depends on the ratio of the height h to the period L. When the condition $h^2/La \geqslant 1$ is met, flat bands arise [10]. Since α that characterizes the deformation of hopping amplitude depends only on h/L, for a given α, increasing height of the ripple would generate flat bands for micron-size ripples. Hence, our results are also applicable to micron-size ripples. For ripples of micron size, the Cooper pair momentum $Q/2$ is smaller. Furthermore, since the energy barrier for realizing the superconducting PDW state is essentially the kinetic energy of the Cooper pair with momentum being $Q/2$, we expect that the energy barrier for realizing the PDW state is lower for ripples of micron size. It is therefore easier to realize the superconducting PDW state in micron-size ripples.

The optimal strain needed to realize the PDW state can be read off from Fig. 4(a) with $\alpha \sim 0.14$, with the corresponding aspect ratio of the ripple being $L/h \approx 20$. The minimum height h thus needs to satisfy $h/L \geqslant 0.05$. Together with the requirement $h^2/La \geqslant 1$, the height requires to realize the PDW state is $h \geqslant 4a$ for $L = 16a$, which can be engineered by appropriate choosing misfit of the thermal expansion between graphene and the substrate [9]. On the other hand, the critical temperature for accessing the PDW state is around 1 meV (a few K) for $J/t = 1$ and is expected to be further reduced for micron-size ripples. Our analyses thus indicate that it is feasible experimentally to realize the long-sought-after superconducting state with nonvanishing center-of-mass momentum for Cooper pairs. Therefore, results of this work illustrate the feasibility for graphene under strain to be a tunable platform for realizing both novel superconducting orders and charge density wave orders.

ACKNOWLEDGMENTS

We acknowledge support from the Ministry of Science and Technology (MoST), Taiwan. In addition,

we also acknowledge support from Center for Quantum Technology, TCECM, and Academia Sinica Research Program on Nanoscience and Nanotechnology, Taiwan.

[1] B. Keimer, S. A. Kivelson, M. R. Norman, S. Uchida, and J. Zaane, Nature (London) **518**, 179 (2015).

[2] J. Bardeen, L. N. Cooper, and J. R. Schrieffer, Phys. Rev. **106**, 162 (1957); J. R. Schrieffer, *Theory of Superconductivity* (Addison Wesley, Redwood City, CA, 1964).

[3] E. Fradkin, S. A. Kivelson, and J. M. Tranquada, Rev. Mod. Phys. **87**, 457 (2015).

[4] P. A. Lee, Phys. Rev. X **4**, 031017 (2014).

[5] N. B. Kopnin, T. T. Heikkila, and G. E. Volovik, Phys. Rev. B **83**, 220503 (2011); V. Khodel and V. Shaginyan, JETP Lett. **51**, 553 (1990); V. J. Kauppila, F. Aikebaier, and T. T. Heikkila, Phys. Rev. B **93**, 214505 (2016).

[6] S. M. Huang, S. T. Lee, and C. Y. Mou, Phys. Rev. B **89**, 195444 (2014).

[7] Y. Cao, V. Fatemi, S. Fang, K. Watanabe, T. Taniguchi, E. Kaxiras, and P. Jarillo-Herrero, Nature (London) **556**, 43 (2018).

[8] Y. Cao, V. Fatemi, A. Demir, S. Fang, S. L. Tomarken, J. Y. Luo, J. D. Sanchez-Yamagishi, K. Watanabe, T. Taniguchi, E. Kaxiras, R. C. Ashoori, and P. Jarillo-Herrero, Nature (London) **556**, 80 (2018).

[9] N. Levy, S. A. Burke, K. L. Meaker, M. Panlasigui, A. Zettl, F. Guinea, A. H. Castro Neto, and M. F. Crommie, Science **329**, 544 (2010); D. Guo, T. Kondo, T. Machida, K. Iwatake, S. Okada, and J. Nakamura, Nat. Commun. **3**, 1068 (2012); For a recent review, see S. Deng and V. Berry, **19**, 197 (2016).

[10] L. Meng, W. Y. He, H. Zheng, M. Liu, H. Yan, W. Yan, Z. D. Chu, K. Bai, R. F. Dou, Y. Zhang, Z. Liu, J. C. Nie, and L. He, Phys. Rev. B **87**, 205405 (2013); N.-C. Yeh, C.-C. Hsu, M. L. Teague, J.-Q. Wang, A. Boyd, and C.-C. Chen, Acta Mech. Sin. **32**, 497 (2016).

[11] L. Tapaszto, T. Dumitrica, S. J. Kim, P. Nemes-Incze, C. Hwang, and L. P. Biro, Nat. Phys. **8**, 739 (2012).

[12] Nonuniform superconducting order parameter was first theorized as the FFLO (Fulde-Ferell-Larkin- Ovchinnikov) state in P. Fulde and R. A. Ferrell, Phys. Rev. **135**, A550 (1964); A. I. Larkin and Yu. N. Ovchinnikov, Sov. Phys.- JETP **20**, 762 (1965). Here the superconducting pair density wave is a realization of periodic superconducting order parameter.

[13] V. M. Pereira, A. H. Castro Neto, and N. M. R. Peres, Phys. Rev. B **80**, 045401 (2009).

[14] This simple realization corresponds to the gauge choice of the vector potential $A_x = 0$, $A_y \neq 0$, for the pseudomagnetic fields induced by the strain. For the results reported in this paper, using more realistic realization of ripples, $t_i = t\exp[-3.37(|\vec{\delta}_i|/a - 1)]$, yields qualitatively the same results.

[15] A. H. Castro Neto, F. Guinea, N. M. R. Peres, K. S. Novoselov, and A. K. Geim, Rev. Mod. Phys. **81**, 109 (2009).

[16] J. V. Sloan, A. A. Pacheco Sanjuan, Z. Wang, C. Horvath, and S. Barraza-Lopez, Phys. Rev. B **87**, 155436 (2013).

[17] R. Jackiw, in *Diverse Topics in Theoretical and Mathematical Physics* (World Scientific, Singapore, 1995), p. 87.

[18] J. E. Hirsch, Phys. Rev. Lett. **54**, 1317 (1985).

[19] M. U. Ubbens and P. A. Lee, Phys. Rev. B **46**, 8434 (1992).

[20] J. X. Li, C. Y. Mou, and T. K. Lee, Phys. Rev. B **62**, 640 (2000); C. T. Shih, T. K. Lee, R. Eder, C. Y. Mou, and Y. C. Chen, Phys. Rev. Lett. **92**, 227002 (2004).

[21] F. C. Zhang, C. Gros, T. M. Rice, and H. Shiba, Supercond. Sci. Technol. **1**, 36 (1988); B. Edegger, V. N. Muthukumar, and C. Gros, Adv. Phys. **56**, 927 (2007).

[22] M. C. Gutzwiller, Phys. Rev. Lett. **10**, 159 (1963).

[23] A. M. Black-Schaffer and C. Honerkamp, J. Phys.: Condens. Matter **26**, 423201 (2014).

[24] D. F. Agterberg and H. Tsunetsugu, Nat. Phys. **4**, 639 (2008).

[25] The coefficients $a(Q)$ and $b(Q)$ can be expressed in terms of integrals over Green's functions; see, for example, R. Soto-Garrido, Y. Wang, E. Fradkin, and S. L. Cooper, Phys. Rev. B **95**, 214502 (2017). In the limit of small Q, both $a(Q)$ and $b(Q)$ are found to be negative.

[26] D. J. Scalapino, S. R. White, and S. C. Zhang, Phys. Rev. B **47**, 7995 (1993).